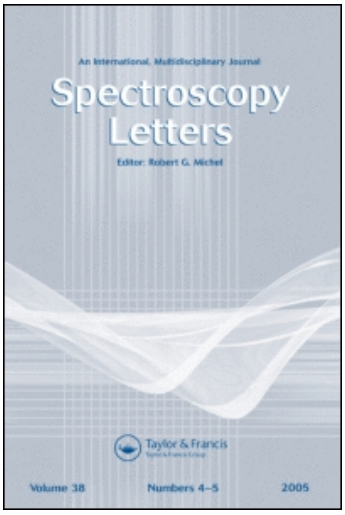

Spectroscopy Letters
Publication details, including instructions for authors and subscription information:
http://www.informaworld.com/smpp/title~content=t713597299

The Infrared and Raman Spectra of β-and α-Tricalcium Phosphate ($Ca_3(Po_4)_2$)

A. Jillavenkatesa[a]; R. A. Condrate Sr.[a]
[a] NYS College of Ceramics, Alfred University, Alfred, NY

To cite this Article Jillavenkatesa, A. and Condrate Sr., R. A.(1998) 'The Infrared and Raman Spectra of β-and α-Tricalcium Phosphate ($Ca_3(Po_4)_2$)', Spectroscopy Letters, 31: 8, 1619 — 1634
To link to this Article: DOI: 10.1080/00387019808007439
URL: http://dx.doi.org/10.1080/00387019808007439

SPECTROSCOPY LETTERS, 31(8), 1619-1634 (1998)

THE INFRARED AND RAMAN SPECTRA OF β- AND α- TRICALCIUM PHOSPHATE ($Ca_3(PO_4)_2$)

KEYWORDS: Tricalcium phosphate, $Ca_3(PO_4)_2$,
Infrared spectra, Raman spectra, Factor Group Analysis

A. Jillavenkatesa and R. A. Condrate, Sr.

NYS College of Ceramics, Alfred University, Alfred, NY 14802

ABSTRACT

Factor group analysis was applied to interpret the vibrational spectra of β- and α- tricalcium phosphate ($Ca_3(PO_4)_2$). The analysis predicts the number of bands formed due to the splitting of the fundamental vibrational modes of the PO_4^{3-} ion. The number of the infrared and Raman bands predicted by this analysis for the two phases are drastically different and can be ascribed to the difference in atomic arrangements in the two phases resulting in greater shielding of the PO_4^{3-} ions in the β- phase than in the α- phase. Discrepancies in the number of predicted and experimentally-observed bands can be attributed to the weak intensities of some vibrational modes or the convolution of vibrations and limited spectral resolution.

INTRODUCTION

Calcium phosphates have been extensively used for dental and orthopedic surgical applications for well over a quarter century [1,2]. Of the numerous phases encountered during processing and characterization of such compounds, tricalcium phosphate ($Ca_3(PO_4)_2$) (TCP), is a phase often generated at higher temperatures (800 °C and above). Formation of tricalcium phosphates is primarily due to the decomposition of other calcium phosphate phases such as hydroxyapatite ($Ca_{10}(PO_4)_6(OH)_2$):

$$Ca_{10}(PO_4)_6(OH)_2 \rightarrow 2\ Ca_3(PO_4)_2 + Ca_4P_2O_9 + H_2O\ . \qquad (1)$$

at elevated temperatures, during sintering of the calcium phosphate green bodies or during plasma spraying operations. This phase is also precipitated as an impurity phase during the preparation of hydroxyapatite by the precipitation process, involving a reaction of calcium nitrate and phosphoric acid [3].

Tricalcium phosphate, characterized with a Ca/P molar ratio of 1.5, possesses two phases, β-$Ca_3(PO_4)_2$ and α-$Ca_3(PO_4)_2$. β-tricalcium phosphate is considered to be the stable phase from room temperature to about 1120 °C, and α-tricalcium phosphate is thermodynamically stable between 1140-1470 °C [4], thus making this phase metastable at room temperature. β-tricalcium phosphate also exhibits bioactive behavior at room temperature, permitting the formation of hydroxyapatite on its surface. Tricalcium phosphate, though closely associated with the processing of hydroxyapatites, exhibits faster dissolution rates than hydroxyapatites in biological fluids. Of the two aforementioned phases, α-tricalcium phosphate dissolves to a greater extent than β-tricalcium phosphate, thus making tricalcium phosphate a useful compound for applications involving temporary support, where regenerated bone replaces the tricalcium phosphate undergoing dissolution. Bone bonding to tricalcium phosphate without a foreign body reaction makes it an attractive material for such applications [5].

Thorough characterization of tricalcium phosphate and the ability to distinguish this phase from other calcium phosphate phases requires a

comprehensive understanding of the vibrational spectra of the different phases of tricalcium phosphate. This study utilizes factor analysis to interpret the Raman and FTIR spectra of β–$Ca_3(PO_4)_2$ and α-$Ca_3(PO_4)_2$, and to correlate the observed bands to suitable molecular vibrations.

EXPERIMENTAL PROCEDURES

A. Preparation of Tricalcium Phosphate.

α-Tricalcium phosphate was processed by a solid state reaction between $CaHPO_4$ (dicalcium phosphate) and $Ca_{10}(PO_4)_6(OH)_2$ (hydroxyapatite), as per the reaction [6] :

$$2\ CaHPO_4 + Ca_{10}(PO_4)_6(OH)_2 \rightarrow 4\ Ca_3(PO_4)_2 + 2\ H_2O. \quad (2)$$

A 2:1 molar ratio batch was thoroughly mixed in a platinum crucible and heated at 1500 °C, in a Molybdenum Disilicide element furnace for 48 hours. At the end of the heat treatment cycle, the sample was quenched in liquid nitrogen in order to retain the α- phase.

β-Tricalcium phosphate used in this study was a high purity commercially available powder (Fluka Chemicals). Powders of both phases were thoroughly crushed to remove any agglomerates, and were characterized using powder X-ray diffraction, Raman and FTIR spectroscopy.

B. X-Ray Diffraction Characterization.

The α- and β- tricalcium phosphate powders were examined for phase purity and crystal structures by powder X-ray diffraction. Samples for XRD characterization were prepared by mounting finely crushed grains on a zero-background holder, and were studied with a Siemens Kristalloflex 810 X-ray diffractometer. The CuK_α radiation applied to study the sample had a wavelength of 0.15412 nm, and was generated under an accelerating potential of 40 kV and a beam current of 30 mA. The diffraction patterns were studied using the *EVA* software package. The powder X-ray diffraction patterns for β- and α- tricalcium phosphate indicate that they are phase pure.

C. Raman and FTIR Spectral Characterization.

The tricalcium phosphate samples were characterized using Raman and FTIR spectroscopy. The mid-IR FTIR spectra of the powders were obtained using a Nicolet 60-SX mid-IR spectrometer, with a CO_2 and H_2O purging system and a resolution of 4.0 cm^{-1}. The spectra were obtained in the transmission mode. Sample pellets were made by mixing 1 mg of the sample powder with 300 mg of dried spectroscopic grade KBr, and pressing in a vacuum die under a pressure of 1200 psi.

Raman spectra of the tricalcium phosphate powders were obtained using an ISA U-1000 Mole double monochromator Raman Spectrometer . The crushed powders were held in a thin walled glass capillary tube of 1 mm inner diameter, and the scattered signal was obtained at a 90° scattering geometry. The incident laser beam was generated from a Coherent Innova 90 Ar^+ -ion laser source had an excitation wavelength of 487.986 nm, and was maintained to generate 100 mW at the sample. The Raman spectrometer was calibrated using the Raman band of TiO_2 observed at 142 cm^{-1}. The spectral resolution of the instrument was 4 cm^{-1}.

RESULTS AND DISCUSSION

A. Phase Stability and Crystal Structure of Tricalcium Phosphate.

Tricalcium Phosphate, melting at approximately 1800 °C is seen to exist over a very wide range of temperatures in three different phases. Of these phases, the commonly encountered ones are, the low temperature β- phase and the high temperature α- phase. The nature of the phases that are present in a material are critically dependent on the calcium to phosphate ratio.

β-Tricalcium Phosphate crystallizes with lattice parameters of the unit cell as a = 1.0439 nm, b = 1.0439nm and c = 3.7375nm. This crystalline phase possesses the rhombohedral space group R3cH-C_{3V}. The unit cell of β-tricalcium phosphate accommodates 21 $Ca_3(PO_4)_2$ molecular units. Based on space group arguments, it has been propounded that there is one formula unit missing from

every unit cell, and this has been associated to the presence of cation vacancies arising from a variation in the cation size to anion size ratio [7].

The stable high temperature α-tricalcium phosphate phase crystallizes as a monoclinic unit cell with the space group P121/a1-C_{2h}. Its unit cell is characterized with lattice parameters of a = 1.2887nm, b = 2.72804nm and c = 1. 5219nm. The unit cell angles are α = 90.0 °, β= 126.2 ° and γ = 90.0 ° [8]. There are 24 formula units per unit cell, and the unit cell consists of columns of cations, and columns of cations and anions with cation vacancies to compensate for the lack of a 2:1 stoichiometric ratio. When compared with the crystal structure of β-tricalcium phosphate, this indicates a striking difference as β-tricalcium phosphate does not possess any cation-cation vacancies (i.e., columns of cation vacancies), but does have cationic sites with half occupancies. Furthermore, α-tricalcium phosphate has a higher percentage of ionic vacancies, giving it a 'looser structure' and greater volume per formula unit. This structural difference has been considered to play a major role in the α–form being the high temperature phase, due to the greater internal energy [8]. A subcell for the α-tricalcium phosphate has been observed where the lattice parameter b" = b/3. This subcell was earlier reported as the structure of α-tricalcium phosphate [9].

B. Spectral Predictions for β- and α- Tricalcium Phosphate.

Considering the crystallographic unit cell of β-tricalcium phosphate, it is observed that 3 Bravais cells constitute its unit cell, and hence, each Bravais cell contains 7 formula units. All of the atoms are accommodated on either C_1 or C_3 symmetry sites in the Bravais cell. From the Wykoff Tables, it is determined that the phosphorous atoms are distributed between these two sites with one set on the C_3 symmetry site, and two sets on the C_1 symmetry sites. All of the oxygen atoms are on the C_1 sites, while the calcium atoms are distributed between the two different sets of sites, the C_1 symmetry sites with three sets of calcium atoms, and C_3 symmetry sites accommodating two sets of calcium atoms.

The structure of β-tricalcium phosphate has been considered to be related to that of $Ba_3(VO_4)_2$, but of a lower symmetry due to the significant differences in the ionic size of barium and calcium [10]. A prominent characteristic of the $Ba_3(VO_4)_2$ structure is the presence of layers of VO_4 groups. However, in the case of the β $Ca_3(PO_4)_2$ structure, similar layers of PO_4 groups are disrupted, and the unit cell is deficient in one PO_4 group. In order to maintain charge balance, a suitable number of calcium ions have to be removed, giving rise to the presence of vacancies in the structure.

Such a presence of vacancies makes it difficult to predict the site occupancies of all of the calcium atoms, and hence, factor group correlation tables and charts cannot be created for calcium atoms. The Fateley method [11] of spectral prediction can be applied to determine the total number of vibrational modes present in the systems. This prediction would include the fundamental internal vibrations and also the translatory and rotatory vibrations. However, this technique has not been applied in this study, due to the limited spectral range of the FTIR and Raman spectrometer. Application of the Winston and Halford [12] technique enables us to calculate the internal vibrational modes characteristic of the phosphate ions in β-tricalcium phosphate. This technique involves the correlation of the free ion group (species with T_d symmetry) through the C_1 and C_3 site groups to the C_{3v} factor group. Table 1 summarizes the spectral splitting due to 3 sets of phosphate ions, with one set occupying the C_3 symmetry site, and 2 equivalent sets accommodated on C_1 symmetry sites.

α-tricalcium phosphate, crystallizing in the monoclinic space group $P12_1/a$, contains 24 formula units per unit cell. This unit cell is the primitive cell, and hence, there are 24 formula units in the Bravais cell. The structure of α-tricalcium phosphate has been compared to that of the mineral glaserite, $K_3Na(SO_4)_2$ [7], due to the presence of similar columns containing cations only and columns containing cation-anion species. Dickens and Brown [13] have described the arrangement of these columns as constituting a pseudohexagonal

Table 1. Resultant Spectral Activity and Coincidences for 1 set of PO_4^{3-} ion on C_3 site and 2 sets of PO_4^{3-} ions on C_1 site for β-$Ca_3(PO_4)_2$.

FUNDAMENTAL MODE DESIGNATION	FREE PO_4^{3-} ION (T_d)	SITE GROUP (C_1)	FACTOR GROUP (C_{2h})
ν_1	1 Raman only A_1	1 IR and Raman A	24 IR only($12A_u+12B_u$) 24 Raman only($12A_g+12B_g$)
ν_2	1 Raman only E	2 IR and Raman 2A	48 IR only($24A_u+24B_u$) 48 Raman only($24A_g+24B_g$)
ν_3	1 IR and Raman F_2	3 IR and Raman 3A	72 IR only($36A_u+36B_u$) 72 Raman only($36A_g+36B_g$)
ν_4	1 IR and Raman F_2	3 IR and Raman 3A	72 IR only($36A_u+36B_u$) 72 Raman only($36A_g+36B_g$)

arrangement, where six cation-anion columns surround each cation column and further, an alternate arrangement of cation-cation and cation-anion columns surround each cation-anion column. The difference between the glaserite and α-tricalcium phosphate structure arises due to the differences in the ionic radii of the ions in the two systems, and also due to the presence of vacancies in α-tricalcium phosphate needed to maintain electroneutrality. These differences cause the cationic columns in α-tricalcium phosphate to be distorted.

Of the two symmetry sites (C_i and C_1) available in this system, it is noted that all of the ions (calcium, phosphate and oxygen) occupy the C_1 symmetry sites. The possibility of phosphate ions being present on the C_i site is ruled out as the C_i site would contain center of symmetry for the phosphate ion, which it does not possess. The presence of oxygen ions on C_i sites can be ruled out on similar center of symmetry arguments. If oxygen ions were to occupy these sites then these ions would have to be equidistant from the phosphate ion which we know is not the case [13]. These C_1 symmetry sites are present in both the cation-cation and cation-anion columns. Thus, there are 18 sets of 4 equivalent calcium ions occupying sites of symmetry C_1, 12 sets of 4 equivalent phosphate ions and 48 sets of 4 equivalent oxygen ions on C_1 symmetry sites. This amounts to a total of 312 atoms in the Bravais cell, which is consistent with the presence of 24 formula units in the Bravais cell.

Considering the splitting of the fundamental vibrational modes specific to the phosphate ion, we see that 12 sets of phosphate ions with each set occupying 4 equivalent C_1 sites lead to splitting of the fundamental vibrational modes such that there are a total of 216 infrared and 216 Raman active internal vibrational modes. None of these vibrational modes are coincident. The predictions for the spectral features due to the factor group splitting of the internal vibrational modes of the phosphate ions in α-tricalcium phosphate considering all the phosphate sites are summarized in Table 2.

Examining the spectral predictions for the factor group splitting of the internal vibrational modes of the phosphate ion, in Tables 1 and 2, we observe

Table 2. Resultant Spectral Activity and Coincidences for 12 sets of PO_4^{3-} ions on C_1 sites for α-$Ca_3(PO_4)_2$.

FUNDAMENTAL MODE DESIGNATION	FREE PO_4^{3-} ION (T_d)	SITE GROUPS		FACTOR GROUP(C_{3v})
		(C_3)	(C_1)	
ν_1	1 Raman only A_1	1 IR and Raman A	1 IR and Raman A	4 IR and Raman $3A_1$+E
ν_2	1 Raman only E	1 IR and Raman E	2 IR and Raman 2A	6 IR and Raman $2A_1$+4E
ν_3	1 IR and Raman F_2	2 IR and Raman A+E	3 IR and Raman 3A	10 IR and Raman $5A_1$+5E
ν_4	1 IR and Raman F_2	2 IR and Raman A+E	3 IR and Raman 3A	10 IR and Raman $5A_1$+5E

that in the case of β-tricalcium phosphate four first-order vibrational bands are predicted. Due to total infrared and Raman coincidence, there are thus, 4 infrared active and 4 Raman active bands, arising due to the splitting of the ν_1 fundamental vibrational mode. In contrast, 24 infrared and 24 Raman bands should be observed for the splitting of the same fundamental mode for α-tricalcium phosphate. The splitting of the ν_2 fundamental vibrational mode gives rise to 6 vibrational bands in β-tricalcium phosphate while the splitting creates 48 vibrational bands in a-tricalcium phosphate. The ν_3 and ν_4 fundamental modes being triple degenerate will have 3 times as many vibrational bands as ν_1, and hence we observe 72 bands in each spectra for each of the triple degenerate fundamental vibrational mode for α-tricalcium phosphate. However, for factor group splitting of the ν_3 and ν_4 fundamental modes creates 10 coincident infrared and Raman bands for each of these modes of β- tricalcium phosphate.

An isolated phosphate ion possesses T_d symmetry and four normal internal vibrational modes. These vibrational modes transform as the irreducible representations $A_1(\nu_1)$, $E(\nu_2)$ and F_2 (ν_3 and ν_4). In the absence of factor group splitting, the ν_1 fundamental mode of the isolated phosphate ion representing the symmetric P-O stretching vibration is characterized by a band at 938 cm^{-1}. The triply degenerate asymmetric P-O stretching mode, (ν_3)is observed at 1017 cm^{-1}. The double degenerate bending mode (ν_2) and the triple degenerate bending mode (ν_4) correspond to the bending vibrations of the O-P-O bond and give rise to bands at 420 and 567 cm^{-1} , respectively [14]. This study has not considered the degree of mixing of the various modes of motion such as, stretching or bending, for the fundamental internal vibrational of both α- and β- tricalcium phosphate. This issue can be addressed by normal coordinate analysis of the systems.

The infrared spectra of α- and β- $Ca_3(PO_4)_2$ is illustrated in figure 1 while their Raman spectra are illustrated in figure 2. Examining the spectra indicates the presence of a greater number of bands than those predicted by the site group model, establishing the inadequacy of this model and necessitating considerations

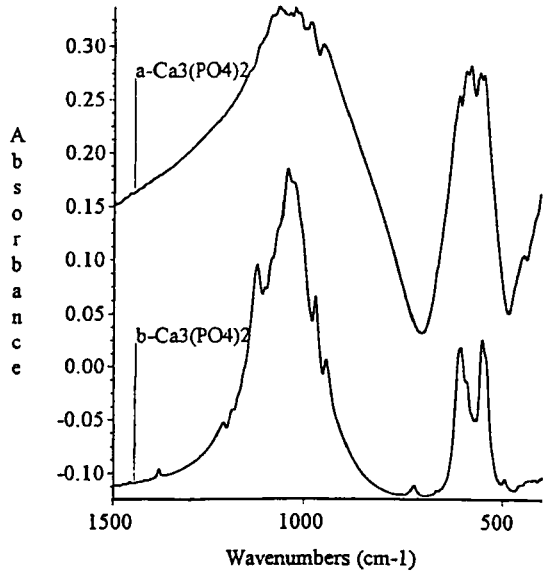

FIG. 1. FTIR spectra of β- and α-$Ca_3(PO_4)_2$.

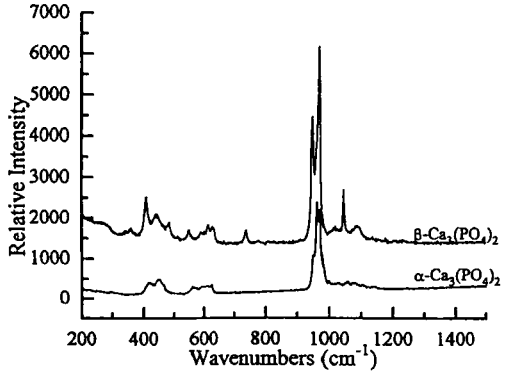

FIG. 2. Raman spectra of β- and α-$Ca_3(PO_4)_2$.

of perturbations due to factor group effects. Further, the apparent coincidence of spectral bands in the infrared and Raman spectra of β-tricalcium phosphate is consistent with the predictions of the applied non-centrosymmetric factor group model. However, in the case of α-tricalcium phosphate, the lack of predicted coincidences is a direct outcome of the centrosymmetric nature of the Bravais cell, illustrating the mutual exclusion principle. Any observed coincidence of vibrational bands in the Raman and infrared spectra are purely accidental. The fewer internal vibrational modes predicted for β-tricalcium phosphate due to factor group splitting indicates weaker splitting effects than those observed in α-tricalcium phosphate. This should be viewed in light of the differences in the atomic arrangements of the two structures, primarily the absence of cation-anion columns in α-tricalcium phosphate, as discussed previously. This results in a larger percentage of vacancies in α-tricalcium phosphate, and hence, in reduced shielding effects on the phosphate ion. The reduced shielding effects in α-tricalcium phosphate are further magnified due to the differences in unit cell volumes of the two phases. The volume per formula unit of α-tricalcium phosphate is18nm^3 while that of β-tricalcium phosphate is 16.8 nm^3.

C. Comparison of Observed Vibrational Spectra with Theoretical Predictions.

A comparison of the spectral predictions for the factor group splitting of the fundamental vibrational modes of the phosphate ion for both α- and β-tricalcium phosphate with the experimentally obtained mid-IR FTIR and Raman spectra of the samples presents a remarkable contrast. The number of bands predicted by the Fateley method and the Winston-Halford technique are far in excess of those observed in the measured spectra. The Raman and FTIR spectra of α-tricalcium phosphate show 17 and 20 distinct bands, respectively. These need to be compared to the non-coincident 216 infrared and 216 Raman bands predicted by the factor group analysis. A similar discrepancy is observed for β-tricalcium phosphate. The experimentally-obtained Raman and FTIR spectra show the

presence of 19 and 21 bands respectively. This is in variance to the 30 infrared and 30 non-coincident Raman bands predicted for the vibrational modes of the phosphate ion.

From figure 2, we observe that the most prominent bands in the Raman spectrum of β-tricalcium phosphate are present at 948 and 970 cm^{-1}. These bands arise due to the factor group splitting of the ν_1 fundamental vibrational mode corresponding to the symmetric P-O stretching vibration of the phosphate ion (938 cm^{-1}). Factor group splitting in the case of α-tricalcium phosphate, however, causes this fundamental mode to split into 3 distinct bands, two strong bands being present at 964 and 976 cm^{-1}, while the third band at 954 cm^{-1} is present as a weak shoulder on the 964 cm^{-1} band, as evidenced in figure 2. Splitting of the same band in the infrared spectrum creates two bands at 972 and 945 cm^{-1} for β-tricalcium phosphate (see figure 1). However, only one band is discernible for α-tricalcium phosphate at this position, namely the band at 954 cm^{-1} (see figure 1). The presence of a band at 984 cm^{-1} in the same spectrum might tempt us to label this band as arising due to the factor group splitting of the ν_1 fundamental vibrational mode, but since factor group splitting requires that the new bands created generally lie within 2-40 cm^{-1} of the fundamental mode, this band has to be assigned as arising due to the splitting of the ν_3 fundamental vibrational mode, corresponding to the triple-degenerate asymmetric P-O stretching mode. The other bands present in this spectrum due to this splitting are at ca. 984, 997, 1013, 1025, 1039 and 1055 cm^{-1}. The Raman spectrum of α-tricalcium phosphate shows the corresponding splitting to create bands at 998, 1012, 1027, 1058 and 1077 cm^{-1}. Referring to the Raman spectrum in figure 2, we see that the splitting of the ν_3 fundamental vibrational mode in β-tricalcium phosphate leads to a very strong distinct band at 1048 cm^{-1} and a weak broad band centered at 1017 cm^{-1}. Strong bands at ca. 1044 and 1025 cm-1 with weak shoulders at ca. 1066 and 1083 cm-1 characterize the corresponding splitting in the infrared spectrum.

In the absence of factor group splitting, the isolated phosphate ion's O-P-O bending vibrations are characterized by bands at 420 and 567 cm^{-1} corresponding to the double-degenerate ν_2 and triple degenerate ν_4 fundamental vibrational mode. Examination of the infrared and Raman spectra of β-tricalcium phosphate (see figures 1and 2) indicates that the band at 420 cm^{-1} splits into very weak bands at 419, 438 458 and 497 cm^{-1} in the infrared spectrum and three distinguishable bands at 406, 442 and 481 cm^{-1} in the Raman spectrum. In case of α-tricalcium phosphate the splitting of the bands of the Raman spectrum at 420 and 567 cm^{-1} is very distinct, as seen in figure 2, and is characterized by bands at 421 and 451 cm^{-1} due to splitting of the 420 cm^{-1} band. Bands at 563, 577, 593, 610 and 620 cm^{-1} arise due to the splitting of the 567 cm^{-1} band. Weak infrared bands in figure 6 at ca. 415, 430, 454, 463 and 471 cm^{-1} arise due to the splitting of the 420 cm^{-1} band and those at ca. 551, 563, 585, 597 and 613 cm^{-1} due to the splitting of the 567 cm^{-1} band. In contrast, the splitting of the infrared band at 567 cm^{-1} of β-tricalcium phosphate gives rise to two strong bands at 555 and 609 cm^{-1}, and a weak shoulder on each of these bands at 544 and 594 cm^{-1}.

From the infrared and Raman spectra of β- and α- tricalcium phosphate we see that the number of bands visible are in variance to the number predicted from the factor group analysis. Coincidences of Raman and infrared bands for β-tricalcium phosphate as predicted by the factor group analysis are not present or obvious, and there are some coincidences observed in the case of α-tricalcium phosphate, contrary to the predictions of the analysis. These discrepancies can be attributed to the convolution of bands that are present too close to be resolved as distinct bands by the spectrometers. In certain instances, it is quite possible that the net change in the polarizability or dipole moment of the vibrational mode may not be strong enough to give rise to a discernible vibrational band in the Raman and infrared spectra, respectively. Such observations can be verified by normal coordinate analysis which help predict the spectral positions of the bands, and thus also address any possibilities of vibrational coupling.

CONCLUSIONS

Factor group analysis of β- and α- tricalcium phosphate predict that the primitive cell of β-tricalcium phosphate should exhibit 30 coincidental Raman and infrared bands for the factor group split internal modes of the PO_4^{3-} ion, while the primitive cell of α-tricalcium phosphate should exhibit 216 Raman and 216 infrared bands for them , of which none should be coincident. More vibrational bands are observed in the infrared and Raman spectra for the internal modes of the PO_4^{3-} ions of the two phases than predicted by the site group models, but less than those predicted by the factor group models. This conclusively establishes the inappropriateness of applying the site group or the free ion model. Differences between the number of observed spectral bands in the experimentally-obtained FTIR and Raman data and those predicted by the factor group analysis arise principally due either to band convolution in the Raman and infrared spectra or to resolution and sensitivity limitations of the spectrometers.

REFERENCES

1. Hench L. L. Bioceramics: From Concept to Clinic, J. Am. Ceram. Soc. 1991; **74:** 1487.

2. Hulburt S. F., Bokros J. C., Hench L. L., Wilson J. and Heimke G. Ceramics in Clinical Applications : Past, Present and Future. In: Vincenzini P. ed. *High Tech Ceramics.* Amsterdam: Netherlands 1987 : 189.

3. Jarcho M., Bolen C. H., Thomas M. B., Bobick J., Kay J. F. and Doremus R. H. Hydroxyapatite Synthesis and Characterization in Dense Polycrystalline Form. J. Mater. Sci. 1988; **23**: 142.

4. Fix W., Heymann H. and Heinke R. Subsolidus Relations in the System $2CaO.SiO_2$ - $3CaO.P_2O_5$. J. Am. Ceram. Soc. 1969; **52:** 346.

5. Doremus R. H. Review: Bioceramics. J. Mater. Sci. Mater. in Med. 1992; **27**: 285.

6. Famery R., Richard N. and Boch P. Preparation of α and β Tricalcium Phosphate Ceramics With and Without Magnesium Addition. Ceramics International 1994; **20**: 327.

7. Dickens B., Schroeder L. W. and Brown W. E. Crystallographic Studies of the Role of Mg as a Stabilizing Impurity in β-$Ca_3(PO_4)_2$. J. Solid. State Chem. 1974; **10**: 232.

8. Mathew M., Schroeder L. W., Dickens B. and Brown W. E. The Crystal Structure of α-$Ca_3(PO_4)_2$. Acta Cryst. 1977; **B33**: 1325.

9. Mackay A. L. A Preliminary Examination of the Structure of α-$Ca_3(PO_4)_2$. Acta Cryst. 1953; **6**: 743.

10. Susse P. and Buerger M. J. The Structure of $Ba_3(VO_4)_2$. Z. Kristallogr. Kristallogeom. Kristallphys. Krystallchem. 1970; **131**: 161.

11. Fateley W. G., McDevitt N. T. and Bentley F. F. Infrared and Raman Selection Rules for Lattice Vibrations: The Correlation Method. Appl. Spec. 1971; **25**: 155.

12. Winston H. and Halford R. S. Motion of Molecules in Condensed Systems: V. Classification of Motions and Selection Rules for Spectra According to Space Symmetry. J. Chem. Phys. 1949; **17:** 607.

13. Dickens B. and Brown W. E. The Crystal Structure of $CaKAsO_4 . 8H_2O$. Acta Crystallogr. Sect. B : Struct. Crystallogr. Cryst. Chem. 1972; **B28:** 3056.

14. Herzberg G. *Molecular Spectra and Molecular Structure II. Infrared and Raman Spectra of Polyatomic Molecules*, New York : D. Van Nostrand Company, Inc., 1945.

Date Received: March 30, 1998
Date Accepted: July 9, 1998